Can Water Trigger Room-Temperature Formation of Benzofuran-2(3H)-one Scaffolds from Vinyldiazene Derivatives? Computational Insights into an Unusual Cyclization

Ulviyya Askerova[d], Yusif Abdullayev*[a,b,c], Namiq Shikhaliyev[b], Avtandil Talybov[c], Jochen Autschbach[f]

[a] Division of Mathematics and Natural Sciences, Allen University, 1530 Harden St. Columbia, SC, 29204, United States. Email: yabdullayev@allenuniversity.edu

[b] Department of Chemical Engineering, Baku Engineering University, Hasan Aliyev str. 120, Baku, Absheron, AZ0101, Azerbaijan.

[c] Institute of Petrochemical Processes, Azerbaijan National Academy of Sciences, Baku AZ1025, Azerbaijan

[d] Organic Chemistry Department, Baku State University, Z. Xalilov str. 23, Az1148, Baku, Azerbaijan

[f] Department of Chemistry, University at Buffalo, State University of New York, Buffalo, New York 14260-3000, United States

Keywords: benzofuran-2(3H)-one, DFT, recrystallization, ring closure

Abstract: Access to benzofuran-2(3H)-one derivatives from readily available substrates under mild conditions is crucial in the pharmaceutical and plastics industries. We identified (Z)-3-(2-phenylhydrazineylidene)benzofuran-2(3H)-one (**P**) during the recrystallization of (E)-2-(2,2-dichloro-1-(phenyldiazenyl)vinyl)phenol using a 96% ethanol solution. The mechanism of the unexpected substrate conversion leading to **P** is investigated using density functional calculations. The computations revealed that ethanol is required to initiate the reaction via **TS1E**, which involves a concerted deprotonation of ethanol by the basic diaza group of the substrate and an ethoxy group attacking the electrophilic center (Cl_2C=), with an energy barrier of 28.3 kcal/mol. The resulting intermediate (**I1E**) is calculated to be unstable and can yield a cyclic chloroacetal adduct with a lower energy barrier of 2.2 kcal/mol via the ring-closure transition state (**TS2E**). In the absence of water, the next steps are impossible because water is required to cleave the ether bond, yielding **P**. A small amount of water (4% of the recrystallization solvent) can promote further transformation of **I2E** via the transition states **TS3E** ($\Delta G‡$ = 11.1 kcal/mol) and **TS4E** ($\Delta G‡$ = 10.5 kcal/mol). A comparison of the ethanol/water- and only water-promoted free energy profiles shows that the presence of ethanol is crucial for lowering the energy barriers (by about 5 kcal/mol) for the initial two steps leading to the cyclic chloroacetal (**I2E**), whereas water is then required to initiate product formation.

Introduction

Benzofuranone derivatives have played a key role in medicinal chemistry because of their effectiveness against lung cancer,[1] their antioxidant potency,[2] and their use as fluorescent probes for imaging sulfite in living cells.[3] Benzofuranone-based polymers have been utilized as a new closed-loop recyclable polymer with enhanced properties exploited as a pressure-sensitive adhesive materials.[4] Benzofuranes can act as enzyme inhibitors, exhibiting α-glucosidase and α-amylase [5] inhibition activities. Structures containing benzofuran scaffold can be found in medicinally important natural products, some of which are shown below:

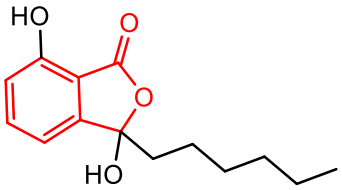

Corollosporine

Immunosuppressive agent

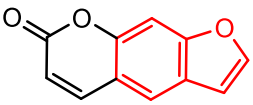

Psoralen

Antifungal

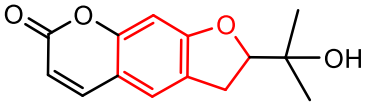

Marmesin

Antimicrobial

In addition to its broad utilization in medicinal applications, the benzofuranone scaffold has been applied as a stabilizer against UV light in the polymer industry under the brand name Irganox® HP-136, which contains 90% benzofuran-2-one (5,7-di-tert-butyl-3-(3,4-dimethylphenyl)3H-benzofuran-2-one): [6]

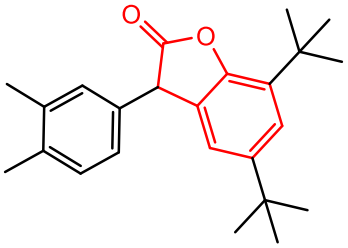

Irganox® HP-136

Stabilizer

The benzofuranone scaffold has therefore become an important target for syntheses in numerous previous works. For instance, it was synthesized using a three-component cascade reaction in the presence of a precious transition metal catalyst $[Cp^*RhCl_2]_2$, an oxidant $(Cu(OAc)_2)$, and an additive (CsOAc) affording the product in low to moderate yields.[7] Benzofuran-2(3H)-one moieties were synthesized via multi-step procedures involving α-arylations of α-diazoacetates.[8] Morita–Baylis–Hillman (MBH) carbonates were converted into the chiral benzofuran-2(3H)-one derivatives using organometallic catalysis.[9] Benzofuran-2(3H)-ones were converted to the enantioenriched 3,3-disubstituted benzofuran-2(3H)-ones using a magnesium-based catalyst.[10] Rh(I)-catalyzed functionalization of the 3-C(sp^3)–H bond of benzofuranones with α-diazoesters resulted in the formation of stereoselective 3-alkylation benzofuranone derivatives. [11] Tong *et al*. also focused on 3-C(sp^3)–H bond functionalization by applying copper (I) catalyst to regioselectively synthesize Z- and E-styrene-containing 3-aryl benzofuran-2(3H)-ones.[12]

We unexpectedly discovered a facile route to benzofuran-2(3H)-one, distinct from the aforementioned employed harsh and/or costly methods. Some of us had previously synthesized dihalogenated heterodienes (vinyldiazenes).[13-15] During the purification of a vinyldiazene derivative, [(E)-2-(2,2-dichloro-1-(phenyldiazenyl)vinyl)phenol], via recrystallization, we observed a color change accompanied by the deposition of dark orange crystals at the bottom of the beaker. This unexpected change motivated us to perform instrumental analyses, including X-ray diffraction, which revealed the spontaneous formation of the benzofuran-2(3H)-one derivative. The experimental procedure, X-ray crystallographic details, and Hirshfeld surface analysis were reported in our previous publications. [16, 17] Subsequently we conducted additional tests, changing the recrystallization solvent from 96% ethanol to absolute ethanol to observe the water role in the benzofuran-2(3H)-one fused ring formation. Surprisingly, we did not identify a trace of the crystals. Utilizing only water as a solvent also did not result in product formation, as the substrate is not soluble in water. A methanol/water mixture can be exploited as a substitute for ethanol/water in the internal cyclization reaction to obtain the product. The observations led us to consider the joint role of water and ethanol vs. the explicit role of water in promoting benzofuran-2(3H)-one formation. We employed density functional theory (DFT) to identify the water, ethanol,

and water/ethanol synergetic impact on the unexpected fused benzofuran-2(3H)-one ring formation reaction in Scheme 1.

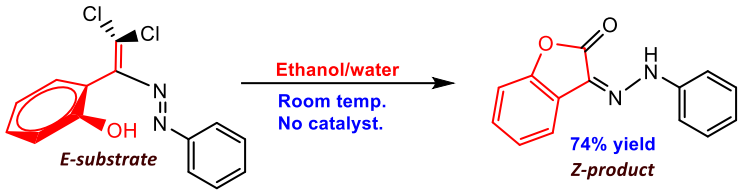

Scheme 1. Ethanol/Water promoted cyclization of (E)-2-(2,2-dichloro-1-(phenyldiazenyl)vinyl)phenol to (Z)-3-(2-phenylhydrazineylidene)benzofuran-2(3H)-one (**P**). The reaction is considered in the DFT studies.

Despite the extensive applications of benzofurans, only a small number of computational studies have been conducted in the past. [18-21]. Therefore, the current research is dedicated to computational mechanistic studies to identify the role of ethanol, water and their synergetic effects on the unexpected cyclization of the aforementioned vinyldiazene derivative.

1. Computational details.

The Gaussian 16 program [22] was used for all calculations. The reaction starting structures, intermediates, transition states and the product were optimized using Kohn-Sham Density Functional Theory (KS-DFT), with the B3LYP functional[23] and D3BJ dispersion corrections.[24] The 6-311G(d,p) basis set was employed for all atoms. Solvent effects were studied using a self-consistent reaction field (SCRF) and default polarizable continuum model (PCM) with the dielectric constant for ethanol (ε= 24.852). Minima and transition states were verified via analytic harmonic vibrational modes, and free energies including entropy contributions from rotations, vibrations, and translations were determined. Gibbs energies and related data are reported for a temperature of 298.15 K to reflect the experimental room temperature conditions. Intrinsic reaction coordinate (IRC) searches were performed to confirm the connections between transition states (TS) and intermediate or product structures.[25] Optimized geometries (in XYZ format), total energies, Gibbs energies, and enthalpies of all structures are provided in the electronic supporting information (ESI, See Tables S1-S4).

2. Results and discussion

The benzofuran-2(3H)-one fused ring formation reaction may be initiated by water, ethanol, or a water/ethanol mixture. The water effects on the substrate cyclization were tested first: As shown in Figure 1, a concerted transition state (**TS1-w**) was identified, representing both deprotonation and the nucleophilic hydroxyl attack on the electrophilic carbon (C1). **TS1-w** is a key transition state that enables a thermodynamically favorable ("downhill") continuation of the reaction via deprotonation (N2-H1, 1.3 Å) and nucleophilic attack on C1 (O1-C1, 1.91 Å), with a 33 kcal/mol energy barrier. Optimization of the intermediate resulting from the IRC calculation (**I1-w**) revealed that the -CCl_2(OH) group is unstable. One of the Cl atoms remains at an extended distance from C1 (Cl1-C1: 1.87 Å), which helps stabilize the structure (See ESI, Figure S3). The Cl1 atom plays a key role in the subsequent ring closure (**TS2-w**) with 7 kcal/mol energy barrier, assisting in the deprotonation of the phenolic hydroxyl group (H2- O2: 1.04 Å and H2-Cl1: 1.84 Å), which facilitates a straightforward nucleophilic attack on C1 (C1-O2: 2:05 Å). **TS2-w** ultimately leads to the formation of **I2-w[HCl]** via HCl extrusion. The remaining chlorine atom (Cl2) attached to C1 facilitates proton removal (H2) via a barrierless **TS3-w**, resulting in the product (**P**) formation (Figure 1).

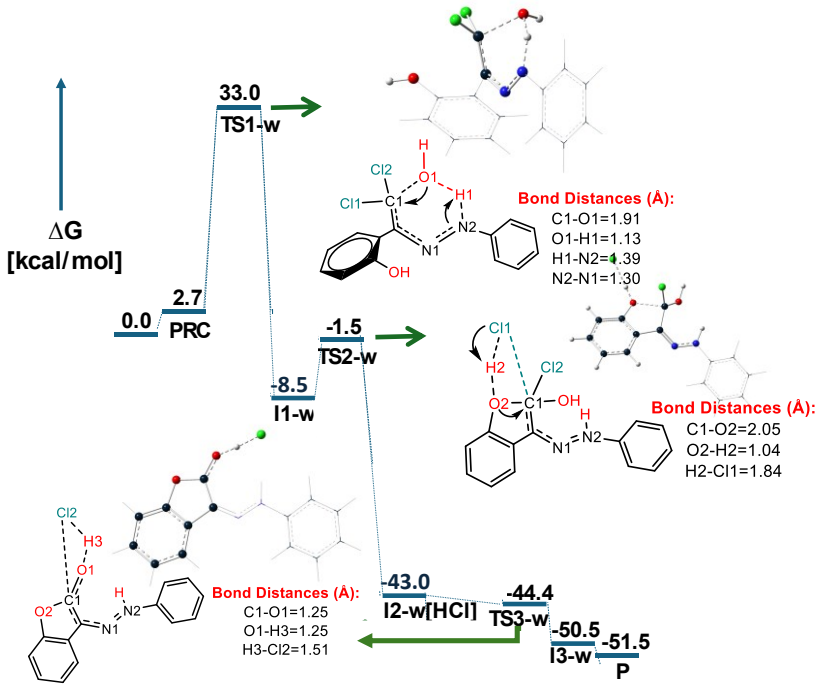

Figure 1. Calculated free energy profile for the water-promoted intramolecular formation of the benzofuran-2(3H)-one fused ring. Transition states (TSs) are illustrated with their geometries and selected interatomic distances (Å).

Besides the reaction starting with water attack from the diaza group side (**TS1-w**) as shown in Figure 1, the reaction may also proceed with water attacking from the opposite side (the phenyl side) on the same electrophilic carbon (C1). Our calculations for this alternative showed that the rate-determining step (**TS1**) requires 49.6 kcal/mol of energy, which is 16.6 kcal/mol higher than that of **TS1-w** (See ESI, Figure S1). As shown in Figure S1, the calculated free energy profile includes an additional three steps with two transition states (36.7 kcal/mol and 43.4 kcal/mol) to yield **P,** which makes the path very unlikely relative to one depicted in Figure 1.

Considering the role of ethanol in the reaction depicted in Scheme 1, we re-calculated the benzofuran-2(3H)-one fused ring formation pathway by including one ethanol molecule in the substrate structure (Figure 2). The similar transition (**TS1E**) state to **TS1-w** was located by replacing the water molecule with ethanol. The ethanol nucleophilic attack (**TS1E**) on the electrophilic carbon (=CCl_2) and the simultaneous deprotonation (transfer of the ethanol hydroxyl proton to the diaza nitrogen) are calculated to have a 28.3 kcal/mol barrier. As shown in Figure 2, the calculated bond distances for the ethanol nucleophilic attack (O1–C1: 1.9 Å) and deprotonation (H1–N2: 1.4 Å) are similar to those calculated in **TS1-w** for the water-mediated attack on the electrophilic C1 (=CCl_2) carbon. Our calculations showed that ethanol lowers the energy barrier by 4.7 kcal/mol compared to **TS1-w**, without altering the transition-state structure. The subsequent step follows a pathway similar to that shown in Figure 1: an important ring-closure transition state (**TS2E**) converts **I1E** into the **I2E** intermediate via Cl2-assisted deprotonation of the phenolic hydroxyl group, followed by nucleophilic attack of the phenolic oxygen (O1) on the electrophilic carbon (C1). This step has a lower energy barrier of 2.2 kcal/mol, which is 4.8 kcal/mol below the corresponding ring-closure step in the water-based **TS2-w**. The calculations indicated that ethanol cannot be utilized further to yield **P**. Therefore, we employed water as a nucleophile to attack on C1 (the electrophilic carbon), generating a carbonyl functionality and hydrolyzing the ether bond to yield **P**. As shown in Figure 2, this step can proceed via the concerted, high-energy transition state **TS3E-C** (ΔG‡ = 52.1 kcal/mol), which is less likely,

or through a stepwise process involving water attack on C1 (O3–C1: 1.63 Å) and water deprotonation (Cl1–H3: 1.7 Å), as depicted in **TS3E**, followed by final ether-bond hydrolysis via proton back-donation from HCl (O1–H3: 1.03 Å) in **TS4E**, with energy barriers of 11.1 kcal/mol and 10.5 kcal/mol, respectively. The final transition state, **TS4E**, converts the semi-acetal form (**I3E**) into the final product through proton transfer (H3–O1: 1.03 Å) from the HCl formed in the previous step, yielding **I4E** and ultimately leading to product (**P**) formation via ethanol and HCl extrusion.

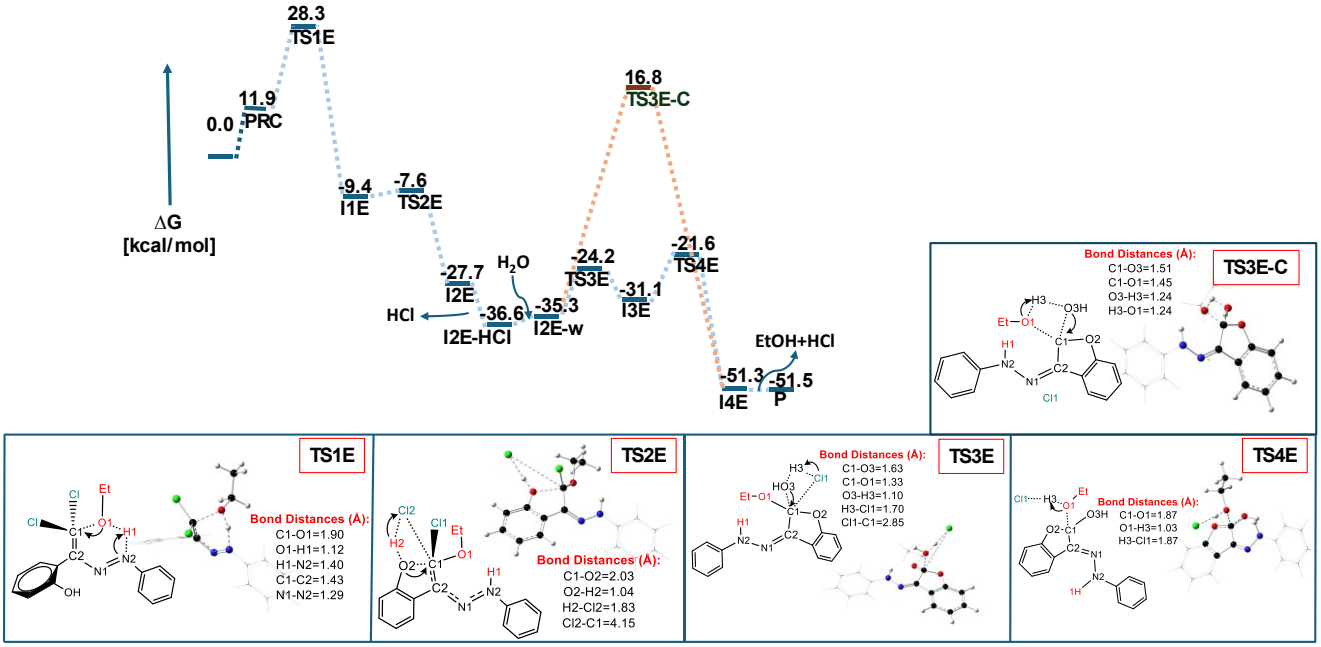

Figure 2. Calculated free energy profile for the ethanol/water-assisted formation of the benzofuran-2(3H)-one fused ring. TSs are shown with their geometries and selected interatomic distances (Å).

Comparing the water-promoted vs. ethanol/water-promoted pathway, it is clear that the latter (Figure 2) is more energetically favorable than in the former (Figure 1). It was determined that ethanol decreases energy barriers for the rate-limiting nucleophilic attack (**TS1E** vs. **TS1-w**), and subsequent ring closure (**TS2E** vs. **TS2-w**) by 4.7 kcal/mol, 4.8 kcal/mol, respectively. Other possibilities were also tested and included in SI which follows considerably higher energy barriers for the ethanol/water profile (Figure S5) requires four steps, each with (**TS1-e**; 44.8 kcal/mol, **TS2-e**; 33.8 kcal/mol, **TS3-e**; 30.1 kcal/mol, and **TS4-e**; 31.8 kcal/mol) to yield **P**. Considering the possibility of a water/ethanol synergistic effect on the nucleophilic attack, we recalculated **TS1-w** of Figure 1 by adding an ethanol molecule in proximity to water. However, this did not yield a transition state with a shallow energy barrier (See SI, Figure S4, **TS1EW**: $\Delta G^{\ddagger}$=34.2 kcal/mol)

Considering that the experimentally observed reaction takes place at room temperature, it appears unlikely that the reaction proceeds via the mechanism shown in Figure 1, since the crucial transition states (**TS1-w**, **TS2-w**) possess higher energy barrier relative to ethanol promoted path (Figure 2). Instead, the ethanol/water-promoted pathway more accurately reflects the experimental conditions, as the alternative transition states (**TS1E**, **TS2E**) exhibit energy barriers approximately 5 kcal/mol lower. Based on our comprehensive investigations, the unexpected formation of fused benzofuran-2(3H)-one in the recrystallization beaker clearly matches the calculated ethanol/water-promoted 'downhill' pathway depicted in Figure 2. The calculated mechanism corresponding to the joint ethanol/water-promoted pathway in Figure 2 is shown in Scheme 2.

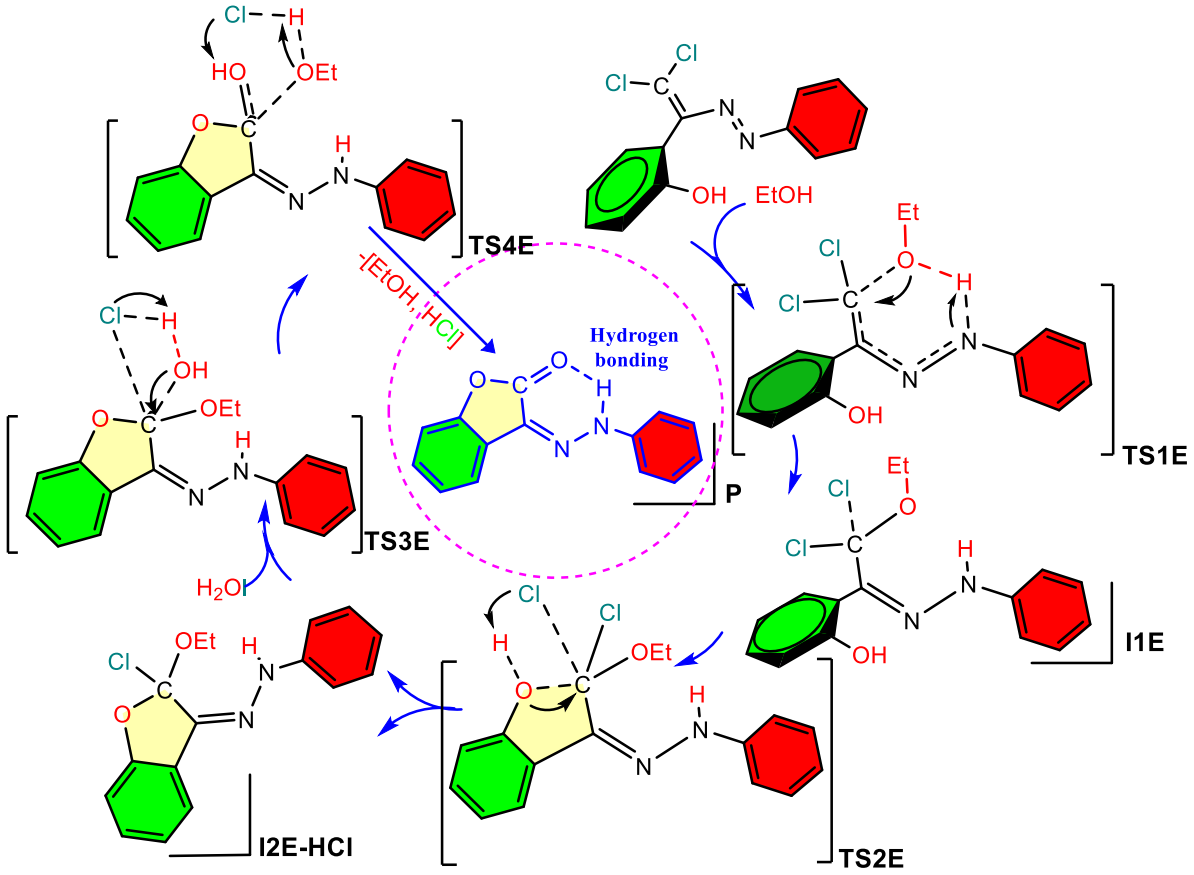

Scheme 2. Calculated mechanism of Figure 2 for the (E)-2-(2,2-dichloro-1-(phenyldiazenyl)vinyl)phenol conversion to (Z)-3-(2-phenylhydrazineylidene)benzofuran-2(3H)-one.

As shown in Scheme 2, rotation around the single (C-N) bond converts the substrate structure to the cis form, which is ideal for ethanol attack (substrate → **I1E**), ultimately resulting in the Z-product (**P**) from E-substrate. Our computational results are in good agreement with the X-ray crystallographic structure of the product (See ESI, Figure S2), which confirms **P** is in Z-form. The theoretically calculated hydrogen bond distance between the NH----O atoms in the **P** structure is 2.04 Å, deviating by only 0.1 Å from the X-ray structure. The presence of the phenolic hydroxyl group is an important influence for the ring closure as depicted in **TS2E** (See Figure 2). The abstraction of the hydrogen atom (H2) by the chlorine atom (Cl2) increases the hydroxyl (O2) nucleophilicity, facilitating its attack on the electrophilic carbon, yielding **I2E**. We performed a control experiment (unpublished) previously, which showed that the formation of such a fused ring product is impossible in the absence of a phenolic hydroxyl group in ortho- position. Likewise, the experiments showed that using a related substrate without the phenolic hydroxyl group resulted in the Z-ester formation. The NMR and X-ray structure of the Z-ester are provided in the ESI (See Figure S6 and S7). We believe that our calculations with the experimental support fully elucidate the role of water and the function of the protic polar solvent (ethanol) in the cyclization of the substrate to form **P**.

Conclusion

DFT calculations were employed to elucidate the unexpected recovery of a benzofuran-2(3H)-one derivative from the recrystallization process intended for substrate purification. The calculated transition state **TS1E**, with an energy barrier of only 28.3 kcal/mol, facilitates the product formation through an ethanol/water-mediated pathway. Our computational studies revealed that the combined effect of water and the recrystallization solvent

(ethanol) plays a key role in the fuse-ring formation. Ethanol helps lower the energy barriers for the rate-determining (**TS1E**) and ring closure (**TS2E**) transition states by about 5 kcal/mol compared to the corresponding transition states (TS1-w and TS2-w) in water-promoted pathway, thereby enabling the reaction to occur at a room temperature. On the other hand, without water, product formation is impossible because, following the second stage of the reaction mechanism, water is needed to initiate nucleophilic attack that removes the ethoxy group in the last two stages (**TS3E** and **TS4E**) of the most feasible pathway shown in Figure 2. Our calculations are in good match with experimental observations, highlighting the ethanol/water unprecedented joint role in facilitating the target reaction to afford fused benzofuna-2(3H)-one ring.

We believe that this finding will contribute to a more facile and environmentally more benign mass production of the benzofuran-2-one scaffold for large-scale applications in the pharmaceutical and plastic industries.

Notes

The authors declare no competing financial interest.

CONFLICTS OF INTEREST

There are no conflicts to declare.

ACKNOWLEDGMENTS

J.A. thanks The National Science Foundation, grant CHE-2152633, for support. All authors thank the Center for Computational Research (CCR, http://hdl.handle.net/10477/79221), University at Buffalo for providing computational resources.

References:

[1] C. Charrier, J. Clarhaut, J.-P. Gesson, G. Estiu, O. Wiest, J. Roche, P. Bertrand, Synthesis and Modeling of New Benzofuranone Histone Deacetylase Inhibitors that Stimulate Tumor Suppressor Gene Expression, Journal of Medicinal Chemistry, 52 (2009) 3112-3115.
[2] M. Fernanda Arias-Santé, J. Fuentes, C. Ojeda, M. Aranda, E. Pastene, H. Speisky, Amplification of the antioxidant properties of myricetin, fisetin, and morin following their oxidation, Food Chemistry, 435 (2024) 137487.
[3] A. Xie, J. Shi, W. Yang, Developing a fluorescent probe containing benzofuranone moiety for imaging sulphite in living hypoxia pulmonary cells, Luminescence, 39 (2024) e4854.
[4] H. Niu, L. Wang, Z. Zhang, Y. Liu, Y. Shen, Z. Li, Ring-Opening Copolymerization of Biorenewable δ-Caprolactone with -Hexahydro-(4,5)-benzofuranone toward Closed-Loop Recyclable Copolyesters and Their Application as Pressure-Sensitive Adhesives, Chinese Journal of Chemistry, 42 (2024) 2035-2042.
[5] C. Deng, N. Zhang, H. Lin, W. Lu, F. Ding, Y. Gao, Y. Zhang, Recent Progress on Natural α-glucosidase Inhibitors Derived from the Plants and Microorganisms, Current Medicinal Chemistry, 31 (2024) 1-27.
[6] A. Mar'in, L. Greci, P. Dubs, Physical behavior of 3-aryl-benzofuran-2-ones (Irganox®HP-136) in polypropylene, Polymer Degradation and Stability, 78 (2002) 263-267.
[7] J. Jiang, J. Liu, Z. Yang, L. Zheng, Z.-Q. Liu, Three-Component Synthesis of Benzofuran-3(2H)-ones with Tetrasubstituted Carbon Stereocenters via Rh(III)-Catalyzed C−H/C−C Bond Activation and Cascade Annulation, Advanced Synthesis & Catalysis, 364 (2022) 2540-2545.
[8] M. Santi, D.M.C. Ould, J. Wenz, Y. Soltani, R.L. Melen, T. Wirth, Metal-Free Tandem Rearrangement/Lactonization: Access to 3,3-Disubstituted Benzofuran-2-(3H)-ones, Angewandte Chemie International Edition, 58 (2019) 7861-7865.
[9] C. Zhu, L. Yang, J. Nie, Y. Zheng, J. Ma, Organocatalytic Asymmetric Branching Sequence of MBH Carbonates: Access to Chiral Benzofuran-2(3H)-one Derivatives with Three Stereocenters, Chinese Journal of Chemistry, 30 (2012) 2693-2702.

[10] D. Li, L. Wang, D. Yang, B. Zhang, R. Wang, Catalytic Desymmetrization of meso-Aziridines with Benzofuran-2(3H)-Ones Employing a Simple In Situ-Generated Magnesium Catalyst, ACS Catalysis, 5 (2015) 7432-7436.
[11] Y. Liu, C. Zhou, M. Xiong, J. Jiang, J. Wang, Asymmetric Rh(I)-Catalyzed Functionalization of the 3-C(sp3)–H Bond of Benzofuranones with α-Diazoesters, Organic Letters, 20 (2018) 5889-5893.
[12] Z. Tong, X. Peng, L. Peng, W. Deng, Z. Wang, H. Lu, W. Yang, S.-F. Yin, N. Kambe, R. Qiu, Cu(I)-Catalyzed C–H Alkenylation of Tertiary C(sp3)–H Bonds of 3-Aryl Benzofuran-2(3H)-ones to Give Z- and E-Styrene Containing Quaternary Carbon Centers with 99/1 Regioselectivity, The Journal of Organic Chemistry, 87 (2022) 6064-6074.
[13] V.G. Nenajdenko, N.G. Shikhaliyev, A.M. Maharramov, K.N. Bagirova, G.T. Suleymanova, A.S. Novikov, V.N. Khrustalev, A.G. Tskhovrebov, Halogenated Diazabutadiene Dyes: Synthesis, Structures, Supramolecular Features, and Theoretical Studies, in: Molecules, 2020.
[14] U. Askerova, Y. Abdullayev, N. Shikhaliyev, A. Maharramov, V.G. Nenajdenko, J. Autschbach, Computational exploration of the copper(I)-catalyzed conversion of hydrazones to dihalogenated vinyldiazene derivatives, Journal of Computational Chemistry, 45 (2024) 2098-2103.
[15] N.G. Shikhaliyev, U.F. Askerova, S.H. Mukhtarova, A.A. Niyazova, P.V. Dorovatovskii, V.N. Khrustalev, V.G. Nenajdenko, Synthesis and Structural Study of Dichlorodiazadienes Derived from 4-Methoxybenzaldehyde, Russian Journal of Organic Chemistry, 56 (2020) 185-192.
[16] Z. Atioglu, M. Akkurt, N.Q. Shikhaliyev, U.F. Askerova, S.H. Mukhtarova, R.K. Askerov, A. Bhattarai, Crystal structure and Hirshfeld surface analysis of 3-[2-(3,5-dimethylphenyl)hydrazinylidene]benzofuran-2(3H)-one, Acta Crystallographica Section E, 77 (2021) 1280-1284.
[17] Z. Atioglu, M. Akkurt, U.F. Askerova, S.H. Mukhtarova, R.K. Askerov, S. Mlowe, Crystal structure and Hirshfeld surface analysis of (3Z)-7-methoxy-3-(2-phenylhydrazinylidene)-1-benzofuran-2(3H)-one, Acta Crystallographica Section E, 77 (2021) 907-911.
[18] C.-C. Wang, Q.-L. Wang, Y.-H. Li, M.-R. Ren, X.-H. Hou, Z.-W. Ma, X.-H. Liu, Y.-J. Chen, Direct Synthesis for Benzofuro[3,2-d]pyrimidin-2-Amines via One-Pot Cascade [4 + 2] Annulation/Aromatization between Benzofuran-Derived Azadienes and Carbodiimide Anions, Chemistry – A European Journal, n/a (2024) e202402886.
[19] G. Kumar, B. Saroha, P. Arya, S. Ghosh, B. Kumari, V.D. Nassare, N. Raghav, S. Kumar, 1,2,3-triazole clubbed and dichloro substituted novel aurones as potential anticancer agents targeting digestive enzymes: Design, synthesis, DFT, ADME and molecular docking studies, Journal of Molecular Structure, 1319 (2025) 139460.
[20] W. Yi, W. Chen, F.-X. Liu, Y. Zhong, D. Wu, Z. Zhou, H. Gao, Rh(III)-Catalyzed and Solvent-Controlled Chemoselective Synthesis of Chalcone and Benzofuran Frameworks via Synergistic Dual Directing Groups Enabled Regioselective C–H Functionalization: A Combined Experimental and Computational Study, ACS Catalysis, 8 (2018) 9508-9519.
[21] M.M. Islam, C.-Z. Wang, X. Feng, S. Rahman, P.E. Georghiou, A. Alodhayb, T. Yamato, Synthesis, Structures and DFT Computational Studies of [3.1.1]Metacyclophanes Containing Benzofuran Rings, ChemistrySelect, 3 (2018) 13542-13547.
[22] M.J. Frisch, G.W. Trucks, H.B. Schlegel, G.E. Scuseria, M.A. Robb, J.R. Cheeseman, G. Scalmani, V. Barone, G.A. Petersson, H. Nakatsuji, X. Li, M. Caricato, A.V. Marenich, J. Bloino, B.G. Janesko, R. Gomperts, B. Mennucci, H.P. Hratchian, J.V. Ortiz, A.F. Izmaylov, J.L. Sonnenberg, Williams, F. Ding, F. Lipparini, F. Egidi, J. Goings, B. Peng, A. Petrone, T. Henderson, D. Ranasinghe, V.G. Zakrzewski, J. Gao, N. Rega, G. Zheng, W. Liang, M. Hada, M. Ehara, K. Toyota, R. Fukuda, J. Hasegawa, M. Ishida, T. Nakajima, Y. Honda, O. Kitao, H. Nakai, T. Vreven, K. Throssell, J.A. Montgomery Jr., J.E. Peralta, F. Ogliaro, M.J. Bearpark, J.J. Heyd, E.N. Brothers, K.N. Kudin, V.N. Staroverov, T.A. Keith, R. Kobayashi, J. Normand, K. Raghavachari, A.P. Rendell, J.C. Burant, S.S. Iyengar, J. Tomasi, M. Cossi, J.M. Millam, M. Klene, C. Adamo, R. Cammi, J.W. Ochterski, R.L. Martin, K. Morokuma, O. Farkas, J.B. Foresman, D.J. Fox, Gaussian 16, Revision C.01, in, Gaussian Inc. Wallingford CT, 2016.
[23] W.J. Hehre, R. Ditchfield, J.A. Pople, J. Chem. Phys., 56 (1972) 2257-2261.
[24] S. Grimme, J. Antony, S. Ehrlich, H. Krieg, A consistent and accurate ab initio parametrization of density functional dispersion correction (DFT-D) for the 94 elements H-Pu, The Journal of Chemical Physics, 132 (2010) 154104.

[25] H.P. Hratchian, H.B. Schlegel, Accurate reaction paths using a Hessian based predictor–corrector integrator, The Journal of Chemical Physics, 120 (2004) 9918-9924.